

## Investigation of electron and hydrogenic-donor states confined in a permeable spherical box using B-splines

T Nikbakht

Department of Physics, Isfahan University of Technology, Iran  
E-mail: tnikbakht@aeoi.org.ir

(Received 10 Jan 2012 , in final form 29 May 2012)

### Abstract

Effects of quantum size and potential shape on the spectra of an electron and a hydrogenic-donor at the center of a permeable spherical cavity have been calculated, using linear variational method. B-splines have been used as basis functions. By extensive convergence tests and comparing with other results given in the literature, the validity and efficiency of the method were confirmed.

**Keywords:** quantum dots, permeable cavity, B-spline technique, potential shape effects

### 1. Introduction

Semiconductor QDs<sup>1</sup> due to their high potential for applications in photonics and quantum information technology have attracted considerable attention since years ago [1]. Performing single dot spectroscopy and using appropriate theoretical models lead to substantial progress in understanding their electronic, optical and spinning properties [2-4]. One of the most important and effective models for studying QDs is the model of confined particles that is used in this paper. This model reconstructs behaviors and characteristics of QDs, properly [5, 6].

Nowadays, researchers can construct nanocrystals in different shapes [7-9]. This requires the study of the quantum confinement effects which in addition to confined quantum systems size depend on their shape, too [10, 11]. Although the single-electron spectrum plays a vital role in the QDs structures, an impurity can change significantly the spectrum of a single-electron under appropriate QDs structures. Impurities in semiconductors affect their optical, electronic and transmission properties [12]. So far, most investigations into the QDs are conducted on impermeable cavities, while permeable cavities are more realistic.

In this paper, spectra of a single-electron and a donor in the center of a permeable spherical cavity with different confinement potentials have been probed. The effects of

potential-shape and quantum-size on the electron and donor spectra have been investigated. Effective atomic units are used throughout this paper. B-splines have been used as basis functions, which can easily perform the trial wave functions with appropriate boundary conditions. B-splines, due to their high efficiency, have been applied successfully to studying various confined quantum systems [11-17]. To learn more about these functions, the reader can refer to [17, 18].

### 2. Model and method

Characteristics of a confined quantum system reflect the form of its confining potential. In this paper, permeable spherical cavity is investigated so that  $V(r)$ , the confining potential, is determined as follows

$$V(r) = \begin{cases} V_0 & \text{if } r \geq R_0 \\ \alpha r^K & \text{if } r < R_0 \end{cases} ; \quad \alpha = \frac{V_0}{R_0^K}, \quad (1)$$

where  $V_0$  is the barrier height of confining potential whose value depends on the desired quantum dot.  $K$  determines the shape of the potential.  $R_0$  is the radius of the permeable cavity. For further information about this confining potential, the reader can refer to [19].

The effective mass approximation is used. Regarding the symmetric potential, we examine the following Schrodinger equation

$$\left[ -\frac{d^2}{2dr^2} + \frac{l(l+1)}{2r^2} - \frac{w}{r} + V(r) \right] U_{n,l}(r) = E_{n,l} U_{n,l}(r), \quad (2)$$

**Table 1.** Convergence of some of the lowest energy levels of a donor in QDs of  $V_0=80\text{au}^*$  and  $R_0=3\text{au}^*$  with  $K=1$ .  $N$  is the number of B-splines for each set of results.

$N$	1s	2s	3s	4s	2p	3p	3d
30	13.2226229	26.7107368	37.4825945	48.1078292	21.8706422	33.3732007	28.6230955
60	13.2225783	26.7078170	37.3013022	46.5307807	21.8387486	33.0335182	28.6170833
90	13.2225765	26.7077392	37.3005911	46.5276773	21.8387342	33.0333438	28.6170390
110	13.2225765	26.7077388	37.3005887	46.5276661	21.8387341	33.0333431	28.6170389

**Table 2.** Convergence of some of the lowest energy levels of a donor in QDs of  $V_0=80\text{au}^*$  and  $R_0=3\text{au}^*$  with  $K=\infty$ .  $N$  is the number of B-splines for each set of results.

$N$	1s	2s	3s	4s	2p	3p	3d
30	-0.4325451	1.0279975	3.5145061	7.0719614	0.4403107	2.3682207	1.2134549
60	-0.4325937	1.0275484	3.5134514	7.0672650	0.4400831	2.3674736	1.2130248
90	-0.4325938	1.0275481	3.5134506	7.0672638	0.4400829	2.3674731	1.2130245
110	-0.4325938	1.0275481	3.5134506	7.0672638	0.4400829	2.3674731	1.2130245

where  $w=0$  and  $w=1$  are for the electron and the donor, respectively. Effective atomic units are used throughout this paper and the length unit is  $1\text{au}^* = 104\text{\AA}$  and energy unit is  $1\text{au}^* = 10.4\text{MeV}$ . Linear variational method is used for solving this problem. For this purpose we have expanded the radial function  $U_{n,l}(r)$ , in terms of B-splines as

$$U_{n,l}(r) = \sum_{i=1}^N c_i^{nl} B_{i,k}(r), \quad (3)$$

where  $B_{i,k}(r)$ , is  $i$  th B-spline of order  $k$ .  $N$  is the number of B-splines used to expand the radial function. Variation of Schrodinger radial wave function is as follows:

$$\left\langle \left( -\frac{d^2}{2dr^2} + \frac{l(l+1)}{2r^2} - \frac{w}{r} + V(r) - E_{n,l} \right) U_{n,l} \middle| B_j(r) \right\rangle = 0 \quad (4)$$

for  $j = 1, \dots, N$

Integral form of the last equation is as follows:

$$\sum_{i=1}^N c_i^{nl} \int_0^R \left[ \frac{1}{2} \frac{dB_i(r)}{dr} \frac{dB_j(r)}{dr} + \left( \frac{l(l+1)}{2r^2} - \frac{w}{r} + V(r) - E \right) B_i(r) B_j(r) \right] dr = 0 \quad (5)$$

for  $j = 1, \dots, N$

Equation (5) is a generalized eigenvalue equation as

$$H_l C = E S C, \quad (6)$$

where  $H_l$  and  $S$  are Hamiltonian and overlap matrixes, respectively. The energy eigenvalues and the corresponding eigenstates can be obtained by diagonalizing the Hamiltonian matrix.

The sequence of the knot points is adopted as

$$\begin{aligned} 0 = t_1 = \dots = t_k < t_{k+1} < \dots < t_j = \dots = t_{j+k-3} \\ = R_0 < \dots < t_{N+k-2} < , \\ t_{N+k-1} = t_{N+k} = R_{\max} . \end{aligned} \quad (7)$$

We use multiple-knot technique to satisfy the boundary conditions.  $N$  is the number of basis functions.  $R_{\max}$  should be chosen large enough to represent the distribution of all desired states. In this paper, for

insurance, we have selected  $R_{\max} = 5R_0$ , although it could be smaller than that. Also,  $k$ , the order of B-splines, is equal to 7.

The numerical-solution program is written in FORTRAN, and the subroutines of ARPACK and LAPACK libraries are exploited for diagonalizing the overlap matrix.

### 3. Results and discussion

Regarding the high localization of B-splines, banded Hamiltonian and overlap matrixes are obtained. Execution time is very short. To check the validity and the efficiency of the method, extensive convergence tests for various shapes of the confining potential have been performed. Some results for some lower energy levels of a donor in a quantum dot of  $V_0=80\text{au}^*$  and  $R_0=3\text{au}^*$  with  $K=1$  and  $K=\infty$ , are shown in tables 1 and 2, respectively. As we can see, the convergence in these states is very fast, especially in the case of  $K=\infty$  (because the potential shape of this case is simpler).

In table 3, we have compared our results for some of the lowest energy levels with those of Zhu et al [19]. Here, following Zhu, our results are normalized with the corresponding value of  $3s$  electron level  $E_{30}(w=0)$  in the QDs. It is noticeable that consistent agreement is achieved. However, there are minor differences between some states. Considering the good convergence of the present method, we believe that our results are reliable.

$K$  determines the shape of the confining potential, therefore according to table 3, energy-level structure alters as  $K$  changes from 1 to  $\infty$ . These changes also are shown in figure 1. As shown in this figure, with  $K$  increasing, the energy levels decrease. Also the potential-shape affects the level ordering. Intersection between levels  $2s$  and  $3d$ ,  $3p$  and  $4f$ , and also  $3s$ ,  $4d$  and  $5g$  together, is shown in figure 1. For  $K$  approximately 7 and above, changes in energy levels become relatively slower and noticeable changes are not observed anymore. So, it can be realized that the potential shape is very impressive on the electronic structure of QDs.

In figure 2, effects of the existence of a donor in QDs on three of the lowest energy levels of a single-electron

**Table 3.** Confined-electron ( $w=0$ ) and confined-donor ( $w=1$ ) spectra normalized by  $E_{30}(w=0)$  for QDs of  $V_0=80a_u^*$  and  $R_0=3a_u^*$ . The data in the brackets are the values obtained by Zhu *et al.* [19]. (The value of  $E_{30}(w=0)$  is equal to 4.6822366, 13.3240493, 23.1900360, 39.1098012 $a_u^*$  for  $K=\infty, 4, 2,$  and  $1,$  respectively).

$K, w$	1s	2p	3d	2s	4f	3p	5g	4d	6h	3s
$\infty, 0$	0.1111621 (0.111)	0.2273989 (0.228)	0.3740937 (0.374)	0.4445730 (0.445)	0.5499046 (0.550)	0.6719899 (0.672)	0.7539510 (0.754)	0.9313124 (0.931)	0.9856003 (0.986)	1.0000000 (1.000)
4, 0	0.1789060 (0.179)	0.3346981 (0.335)	0.5105117 (0.511)	0.5482880 (0.548)	0.7026626 (0.703)	0.7548913 (0.755)	0.9087907 (0.909)	0.9719886 (0.972)	1.1272343 (1.069)	1.0000000 (1.000)
	1s	2p	2s	3d	3p	4f	3s	4d	5g	4p
2, 0	0.2727272 (0.273)	0.4545454 (0.455)	0.6363636 (0.636)	0.6363636 (0.636)	0.8181818 (0.818)	0.8181818 (0.818)	1.0000000 (1.000)	1.0000000 (1.000)	1.0000000 (1.000)	1.1818182 (1.182)
1, 0	0.4235272 (0.424)	0.6088612 (0.609)	0.7404954 (0.740)	0.7695202 (0.770)	0.8847747 (0.885)	0.9149210 (0.915)	1.0000000 (1.000)	1.0197713 (1.020)	1.0496078 (1.050)	1.1244554 (1.124)
	1s	2p	2s	3d	4f	3p	5g	3s	4d	6h
$\infty, 1$	-0.0923904 (-0.095)	0.0939899 (0.093)	0.2194567 (0.217)	0.2590694 (0.258)	0.4439460 (0.443)	0.5056287 (0.504)	0.6535648 (0.653)	0.7503787 (0.748)	0.7885307 (0.787)	0.8890518 (0.888)
4, 1	0.0486118 (0.031)	0.2476780 (0.237)	0.4239191 (0.408)	0.4383877 (0.429)	0.6387755 (0.631)	0.6661546 (0.655)	0.8503619 (0.843)	0.8808049 (0.866)	0.8979240 (0.889)	1.0727882 (1.012)
	1s	2p	2s	3d	3p	4f	3s	4d	5g	4p
2, 1	0.1653816 (0.143)	0.3863370 (0.373)	0.5504602 (0.534)	0.5824043 (0.572)	0.7573396 (0.746)	0.7721398 (0.763)	0.9244720 (0.910)	0.9500717 (0.941)	0.9591693 (0.951)	1.1258022 (1.115)
1, 1	0.3380886 (0.314)	0.5583954 (0.545)	0.6828912 (0.667)	0.7317102 (0.722)	0.8446308 (0.834)	0.8839806 (0.876)	0.9537402 (0.941)	0.9876396 (0.976)	1.0230634 (1.016)	1.0901302 (1.081)

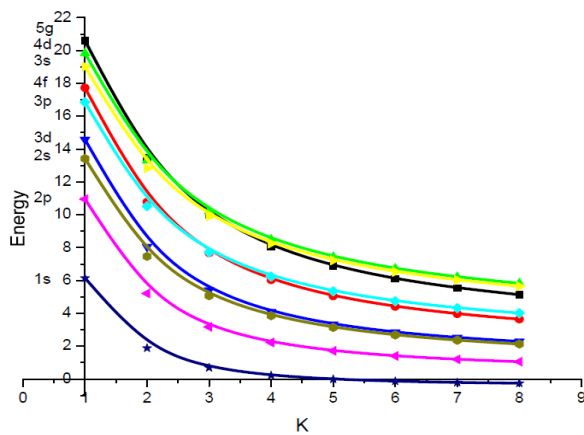


**Figure 1.** Energy levels of a donor in QDs of  $V_0=30a_u^*$  with  $R_0=3a_u^*$  as a function of  $K$ .

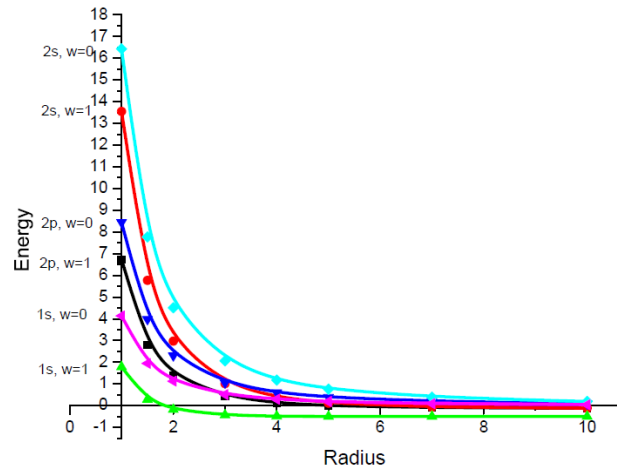


**Figure 2.** Comparison between the three lowest energy levels of a donor ( $w=1$ ) and a single-electron ( $w=0$ ) in QDs of  $V_0=60a_u^*$  with  $K=\infty$  as a function of  $R_0$ .

**Table 4.** Energy levels of a donor in QDs of  $V_0=60a_u^*$  with  $K=\infty$ .

$R_0$	1s	2s	3s	2p	3p	3d	4d	4f	5g
1.0	1.7815534	13.5527327	33.2569790	6.7341397	22.5814812	12.3698602	32.2189966	18.9546995	26.5025159
2.0	-0.1788754	2.9713530	8.4214575	1.4000333	5.6738219	3.0062008	8.4564884	4.8487660	6.9539245
3.0	-0.4338350	1.0150885	3.4801252	0.4340103	2.3452376	1.2011866	3.6594087	2.0600418	3.0336823
4.0	-0.4854313	0.3839526	1.7696202	0.1258778	1.1920808	0.5845781	1.9651491	1.0840227	1.6453125
5.0	-0.4968957	0.1252038	1.0029057	-0.0002508	0.6736623	0.3113255	1.1879801	0.6401268	1.0061699
7.0	-0.4998822	-0.0552678	0.3758642	-0.0894981	0.2465598	0.0908974	0.5278011	0.2676331	0.4602550
10.0	-0.4999994	-0.1134570	0.0868808	-0.1191941	0.0459911	-0.0086339	0.1968319	0.0852079	0.1836115
20.0	-0.5000000	-0.1249880	-0.0500859	-0.1249950	-0.0517311	-0.0540184	-0.0059950	-0.0202162	0.0085733

spectrum are shown. Energy levels of a donor and a single-electron in QDs of  $V_0=60a_u^*$  with  $K=\infty$  is shown in tables 4 and 5, respectively. It is seen in figure 2 and by comparing table 4 with table 5 that the existence of a donor in QDs decreases the corresponding energy levels of the single-electron. With  $R_0$  decreasing, the differences

between corresponding energy levels increase. Also, as shown in table 3, the introduction of a donor changes the ordering of  $s$  and  $d$  states. This phenomenon depends on the potential shape and for different  $K$ , the ordering of the levels is not the same. Therefore, the existence of a donor in QDs, effectively changes the energy levels.

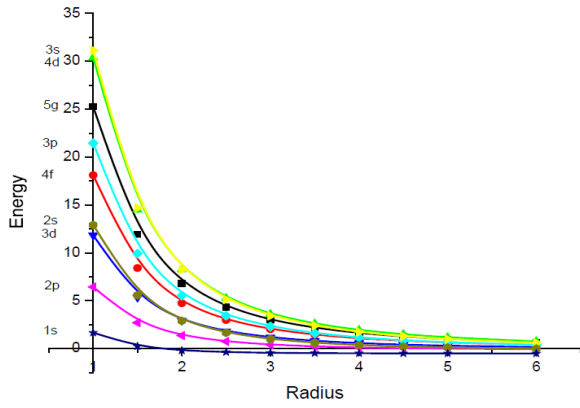


**Figure 3.** Energy levels of a donor in QDs of  $V_0=40au^*$  with  $K=\infty$  as a function of  $R_0$ .

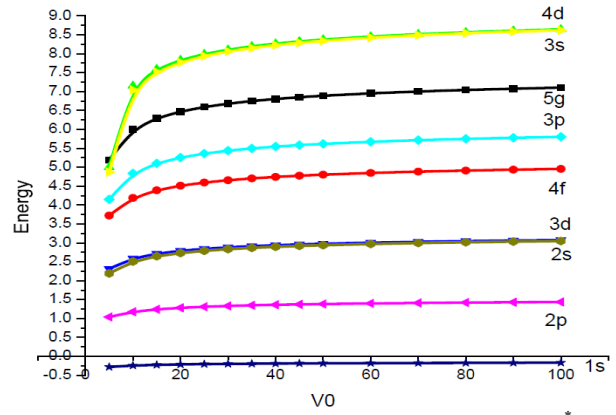


**Figure 4.** Energy levels of a donor in QDs of  $R_0=2au^*$  with  $K=\infty$  as a function of  $V_0$ .

**Table 5.** Energy levels of a single-electron in QDs of  $V_0=60au^*$  with  $K=\infty$ .

$R_0$	1s	2s	3s	2p	3p	3d	4d	4f	5g
1.0	4.1355232	16.4305840	36.3969861	8.4453064	24.7153550	13.8659144	34.0476472	20.3364751	27.8108180
2.0	1.1280351	4.5082806	10.1281188	2.3071314	6.8114301	3.7946692	9.4354303	5.5767690	7.6442159
3.0	0.5163618	2.0649123	4.6439835	1.0562702	3.1210211	1.7376217	4.3251691	2.5541677	3.5018025
4.0	0.2948044	1.1790868	2.6524466	0.6030769	1.7823026	0.9921390	2.4701941	1.4584372	1.9996425
5.0	0.1903734	0.7614501	1.7130972	0.3894499	1.1510431	0.6407055	1.5953523	0.9418490	1.2913797
7.0	0.0981333	0.3925251	0.8831501	0.2007549	0.5933723	0.3302767	0.8224368	0.4855186	0.6657082
10.0	0.0484593	0.1938356	0.4361247	0.0991352	0.2930199	0.1630954	0.4061405	0.2397571	0.3287393
20.0	0.0122276	0.0489105	0.1100484	0.0250147	0.0739380	0.0411537	0.1024822	0.0604978	0.0829509

**Table 6.** Energy levels of a donor in QDs of  $R_0=3au^*$  with  $K=\infty$ .

$V_0$	1s	2s	2p	3p	3d	4d	4f
20	-0.4402094	0.9491887	0.4020697	2.2261012	1.1384835	3.4824757	1.9608973
40	-0.4358642	0.9944794	0.4239864	2.3082820	1.1815936	3.6048938	2.0291652
60	-0.4338350	1.0150885	0.4340103	2.3452376	1.2011866	3.6594087	2.0600418
80	-0.4325938	1.0275481	0.4400829	2.3674731	1.2130245	3.6920875	2.0786603
100	-0.4317329	1.0361292	0.4442701	2.3827460	1.2211741	3.7144886	2.0914640
$\infty$	-0.4239673	1.1116847	0.4812503	2.5162090	1.2928033	3.9092421	2.2036554

In figure 3 the energy levels of a donor in QDs of  $V_0=40au^*$  with  $K=\infty$  are shown as a function of  $R_0$ . It is readily seen that with  $R_0$  increasing, the energy levels decrease. Also,  $R_0$  has obvious effects on the ordering. For example, the crossover of  $2s$ ,  $3d$ , and  $3s$  with  $4d$  states occurs as  $R_0$  changes. These kinds of changes are observable from table 4, too. As QDs get bigger, the values of energy levels tend to constant numbers that are approximately the energy levels of the free relevant particle.

In table 6, energy levels of a donor in QDs of  $R_0=3au^*$  with  $K=\infty$  are shown for different values of  $V_0$ . In figure 4 we have plotted the energy levels of a donor in QDs of  $R_0=2au^*$  with  $K=\infty$ , as a function of  $V_0$ . In fact, the amount of  $V_0$  depends on the desired quantum dot. It is seen that with  $V_0$  increasing, the energy levels increase, too. In this case, higher levels undergo more changes than lower levels that mean  $V_0$  affects higher levels more than lower levels. For  $V_0$  approximately  $30au^*$  and above, the values of energy levels undergo negligible changes. According to figure 4, some levels, like  $2s$ ,  $3d$  and  $3s$ ,  $4d$  are approximately corresponding to one another.

### 4. Summary

In this paper, we have examined the spectra of a single-electron and a donor in the center of a permeable cavity, using B-splines. The variational approach we employed here produced energy eigenvalues with high accuracy at low computational cost. We tried to precisely obtain the effects of quantum-size and potential-shape on the spectra of a single-electron and a donor in the center of a permeable spherical cavity. The size and shape effects on the low-lying states were probed. Also, the effects of a present donor on the single-electron spectrum in QDs were investigated. Considering these effects was useful in electronic device applications.

Due to diverse and new forms of QDs, studying the confined quantum systems with different shapes has attracted considerable attention over the last decade. Regarding the validity and the efficiency of the method applied here, we can extend it to investigate QDs with more realistic shapes.

**References**

1. M Kroutvar, Y Ducommun, D Heiss, M Bichler, D Schuh, G Abstreiter, and J J Finley, *Nature* **432** (2004) 81.
2. E Baudin, E Benjamin, A Lemaître, and O Krebs, *Phys. Rev. Lett.* **107** (2011) 197402.
3. V Loo, L Lanco, O Krebs, P Senellart, and P Voisin, *Phys. Rev. B* **83** (2011) 033301.
4. M N Makhonin, E A Chekhovich, P Senellart, A Lemaître, M Skolnick, and A I Tartakovskii, *Phys. Rev. B* **82** (2010) 161309.
5. S Goldman, and C Joslin, *J. Phys. Chem.* **96** (1992) 6021.
6. V K Dolmatov, A S Baltenkov, J P Connerade, and S T Manson, *Rad. Phys. And Chem.* **70** (2004) 417.
7. L Manna, E C Scher, and A P Alivisatos, *J. Am. Chem. Soc.* **122** (2000) 12700.
8. V F Punters, K M Krishnan, and A P Alivisatos, *Science* **291** (2001) 2115.
9. X Peng, L Manna, W Yang, J Wickham, E Scher, A Kadavanich, and A P Alivisatos, *Nature* **404** (2000) 59.
10. X Z Li and J B Xia, *Phys. Rev. B* **68** (2004) 165316.
11. S Kang, Q Liu, H Y Meng, and T Y Shi, *Phys. Lett. A* **360** (2007) 608.
12. Sh Kang, J Li, and T Y Shi, *J. Phys. B: At. Mol. Opt. Phys.* **39** (2006) 3491-3505.
13. P Hui, T Y Shi, and Ch G Bao, *Commun. Theor. Phys.* **39** (2003) 341.
14. T Y Shi, H X Qiao, and B W Li, *J. Phys. B: At. Mol. Opt. Phys.* **33** (2000) 349.
15. S Kang, Y M Liu, and T Y Shi, *Eur. Phys. J. B* **63** (2008) 37.
16. M Barezi, T Nikbakht, *Iranian Journal of Physics Research* **10** (2011) 309.
17. H Bachau, E Cormier, P Decleva, J E Hansen, and F Martin, *Rep. Prog. Phys.* **64** (2001) 1815.
18. C deBoor, "A Practical Guide to Splines", Springer-Verlag, New York (1978).
19. J L Zhu, J Wu, R T Fu, H Chen, and Y Kawazoe, *Phys. Rev. B* **55** (1997) 1673.